Mem. S.A.It. Suppl. Vol. 25, 86

Memorie della
Supplementi

Corrugated velocity patterns in the spiral galaxies: NGC 278, NGC 1058, NGC 2500 & UGC 3574

M. C. Sánchez Gil[1], E. J. Alfaro[2], and E. Pérez[2]

[1] Universidad de Cádiz, Facultad de Ciencias Poligono Rio San Pedro 11510 - Puerto Real, Spain, e-mail: mcarmen.sanchez@uca.es
[2] Instituto de Astrofísica de Andalucía (CSIC), E18008, Granada, Spain

Abstract. In this work we address the study of the detection in Hα of a radial corrugation in the vertical velocity field in a sample of four nearly face-on, spiral galaxies. The geometry of the problem is a main criterion in the selection of the sample as well as of the azimuthal angle of the slits. These spatial corrugations must be equally associated with wavy vertical motions in the galactic plane with a strong large-scale consistency. Evidence of these kinematic waves were first detected in the analysis of the rotation curves of spiral galaxies (eg Vaucoleurs & de Vaucaleurs 1963, Pismis 1965), but it was not until 2001 that Alfaro et al. analyzed in more detail the velocity corrugations in NGC 5427 and a possible physical mechanism for their origin. The aim of this study is to analyze the corrugated velocity pattern in terms of the star formation processes. We describe the geometry of the problem and establish its fundamental relationships.

Key words. Techniques: spectroscopic–Galaxies: kinematics and dynamics - spiral - structure

1. Introduction

The disks of spiral galaxies are highly structured. Besides the spiral arms typically associated to the galaxy main plane, there are systematic deviations, above and below the plane, which show characteristic patterns. The sinusoidal wave-like morphologies, observed first in the gas component of the Milky Way, have been called *corrugations* (ie Gum, Kerr & WesterVerschuur 1973, Morton 1965, Lockman 1977). Corrugations have been also observed in the stellar population of the Milky Way (ie Quiroga 1977, Alfaro, Cabrera-Cao & Delgado 1992) and both in the azimuthal direction along different spiral arms (Spicker & Feitzinger 1986), as in the radial, in different galactocentric radii (Malhotra & Rhoads 1995). This phenomenology is not just limited to our Galaxy but has also been observed in external galaxies (eg Florido et al. 1991, Matthews & Uson 2008) and for different tracers of both gas and stellar population. Thus, although most of the stellar corrugations were determined from the distribution of young stars, infrared observations seem to show that the old stellar population also participates in this structure (Djorgowski & Sosin 1989, Rhoads 1995). All these results

Send offprint requests to: M. C. Sánchez Gil suggest that this is a universal phenomenon presents in any late-type galaxy, observable in almost any wavelength (Alfaro & Efremov 1996, Matthews & Uson 2008). A universal phenomenology, barely studied and poorly understood.

Clearly, these spatial corrugations must be equally associated with wavy vertical motions in the galactic plane with a strong large-scale consistency. Evidence of these kinematic waves were first detected in the analysis of the rotation curves of spiral galaxies (eg Vaucouleurs & de Vaucouleurs 1963, Pismis 1965), but it was not until 2001 that Alfaro et al. analyzed in more detail the velocity corrugations in NGC 5427 and a possible physical mechanism for their origin. Given the nature of the problem, galaxy-observer geometry plays a fundamental role in the interpretation of the observables. Thus, from within our galaxy we can easily observe the corrugated structure of the spiral arms in the solar neighborhood in the optical range and large-scale structure of HI, while the vertical velocity field of these morphologies shows a component almost null in the direction of the line of sight. By contrast, the face-on external galaxies represent the best natural laboratory for the study of the corrugations of the velocity field, given that most of the observed radial velocity is representative of the vertical component of velocity, but do not provide any information about spatial corrugations.

Many theories have been proposed to explain this phenomenon (see Alfaro & Efremov 1996; Alfaro 2003), however, there has been no systematic study of this phenomenology to collect a homogeneous data set that would refute which physical mechanism or mechanisms are mainly responsible for these structures.

2. Galaxy sample and data

The sample consists of four nearly face-on, spiral galaxies. The geometry of the problem is a main criterion in the selection of the sample as well as the azimuthal angle of the slits. The sample is made from the LEDA database (Lyon-Meudon Extragalactic Database), where the selection criteria are: low inclination angle (i< 25°); nearby (v < 4000kms^{-1}); a well defined spiral morphological type (2<t<8); and a diameter larger than 2 arcmin (D_{25} > 2). This information and other basic properties of the galaxy sample are summarized in Table 1.

Figure 1 shows NGC 2500, where an HST image is represented together the different slit positions, as well as an Hα image, taken from the LVL survey, plotted with contours levels. The reference point corresponds to the galactic center. In Table 1 are summarized the main characteristics of the sample galaxies.

We obtained long-slit spectroscopy with the double arm ISIS spectrograph attached to the 4.2m William Herschel Telescope (WHT), at the Roque de los Muchachos Observatory (La Palma) during December 2003. Two spectral ranges observed simultaneously, a blue one centered around Hβ (4861 Å), and a red one around Hα (6563 Å). The gratings used, R1200R and R600B, provide a dispersion of 0.23 and 0.45 Å/pixel respectively. The slit width of 1 arcsec projects onto about 3.64 pixels Full-Width-Half-Maximum on the detector; the spatial sampling along the slit is 0.2"/pixel. The slit was placed at two or three different position angles for each galaxy.

3. V_Z calculation

In the case of just face-on galaxies the vertical component of the velocity disk field should be straightforward obtained. The observed velocity is assumed as the result of the sum of the projected vertical and the parallel components to the disk, due to their inclination angle: $V_{obs} = V_{sys} + [V_{\parallel} \sin i + V_{\perp} \cos i] = V_{sys} + [(V_{rot} \cos\theta + V_{exp} \sin\theta) \sin i + V_Z \cos i]$, where V_{sys} is the systemic velocity of the galaxy, V_{rot} and V_{exp} the rotational and expansion velocity respectively, at the plane of the disk, and V_Z is the vertical velocity component. θ is the angle in the plane of the galaxy (counterclockwise from the major axis), and i is the inclination angle of the galaxy disk.

Considering the relation between the polar coordinates in the plane of the sky, (r,ϕ), and in the plane of the galaxy, (R,θ) : $R = r(\cos^2(\phi - PA) + \sin^2(\phi - PA) \cos^{-2} i)^{1/2}$; $R \cos\theta = r \cos(\phi - PA)$; and $R \sin\theta =$

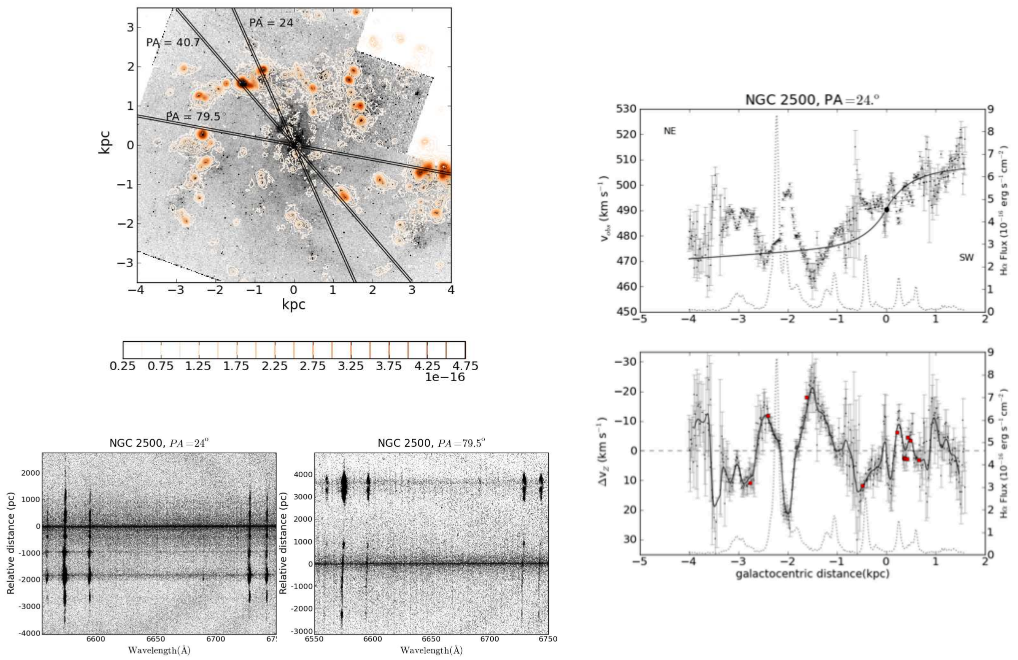

Fig. 1. *Left:* On the top an HST image (WFPC2 instrument and F450W filter) of NGC 2500 - North up, East left-, together the three different slit positions. An Hα image, taken from the LVL survey, is also plotted with contours levels, from 2.5E-17 to 5.E-16 erg/s/cm^2, in an orange color code of the flux-scale; On the bottom, bi-dimensional spectra centered at Hα, [NII] and [SII]. *Right:* Top panel: V_{obs}, together the V_{rot} (black line) and the V_{sys} of the galaxy (black circle), in front of the galactocentric distance. Zero marks the galactic center. Hα emission line flux is also plotted, dashed lines. Bottom panel: the perpendicular velocity ΔV_Z, obtained as described in Section 3.

$r\sin(\phi - PA)\cos^{-1} i$. And neglecting the expansion velocity, $V_Z = \left(V_{obs} - V_{sys} - V_{rot}\frac{\sin i}{\sqrt{1+\tan^2(\phi-PA)/\cos^2 i}}\right)\cos^{-1} i$ [1]. The vertical velocities are computed then as a function of V$_{sys}$, V_{obs}, ϕ, the corresponding slit position angle, V$_{rot}$, PA the position angle of the line of nodes, and i. Data for the rotation curves, inclination angles and PAs for each galaxy are taken from Epinat et al. (2008), see Table 1.

Finally, V_Z shows some residual trend which seems to be mainly related with the rotational velocity removal, see Figs. 1&2. To remove these rotational residues, the vertical velocity component has been detrended, ΔV_Z, by fitting a linear component to the gentle rise for each rotation curve side, the approaching and the receding sides.

4. Results

The aim of this work is to show the existence of systemic perpendicular motions, as well as giving a description of its morphologies or patterns. The maxima and minima values of V_Z are related with Hα emission line peaks, and with the morphology of the galaxy. We describe the observed phenomenon, interpreted as perpendicular movements or velocities with respect the galactic disk, V_Z, of the ionized gas

Table 1. Galaxy Parameters[a]

Galaxy	RA (J2000) h m s	Dec. (J2000) ° ′ ″	Type	Redshift	Dist.[b] (Mpc)	Inclin.[c] (deg)	PA[c] (deg)	Dimensions (arcmin)	M_B
NGC 278	00 52 04.3	+47 33 02	SAB(rs)b	0.002090	12.1	21±14	52± 3	2.1×2.0	-19.6
NGC 1058	02 43 30.0	+37 20 29	SA(rs)c	0.001728	9.8	6 ± 15	125± 6	3.0×2.8	-18.7
UGC 3574	06 53 10.4	+57 10 40	SA(s)cd	0.004807	21.8	19 ± 10	99± 3	4.2×3.6	-18.0
NGC 2500	08 01 53.2	+50 44 14	SAB(rs)d	0.001715	11.0	41± 10	85± 2	2.9×2.6	-18.2

[a] Sourced from *NASA Extragalactic Database*; [b] Moustakas & Kennicutt 2006; James et al. 2004; [c] Epinat et al. 2008.

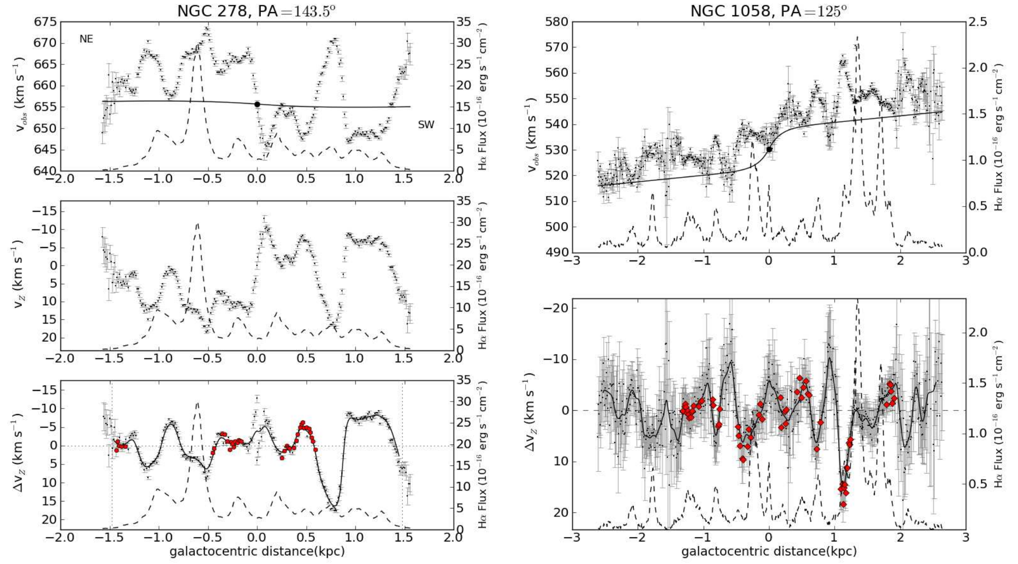

Fig. 2. Top panels: V_{obs}, together the V_{rot} (black line) and the V_{sys} of the galaxy (black circle), in front of the galactocentric distance. Zero marks the galactic center. Hα emission line flux is also plotted, dashed lines. Bottom panels: V_Z and ΔV_Z, obtained as described in Section 3. The red filled circles show those locations where some traces of shocks are found in the Diagnostic Diagrams.

component. At Figs. 1 and 2, some representative examples of the calculated V_Z are showed.

We found different behaviors of the vertical velocity component respect to the Hα emission peaks, for our galaxy sample. In some slit positions of NGC 278, NGC 1058 and NGC 2500 plots, we find a systematic displacement between the velocities and emission line peaks. This displacement is very similar to that observed in NGC 5427 (Alfaro et al. 2001), where the approaching (negative values) peaks of ΔV_Z occur in the convex border of the arms, and the receding maxima (positive values) are located behind the Hα emission maxima, in the concave side. This kinematical behavior is similar to the response of a gas flow into a

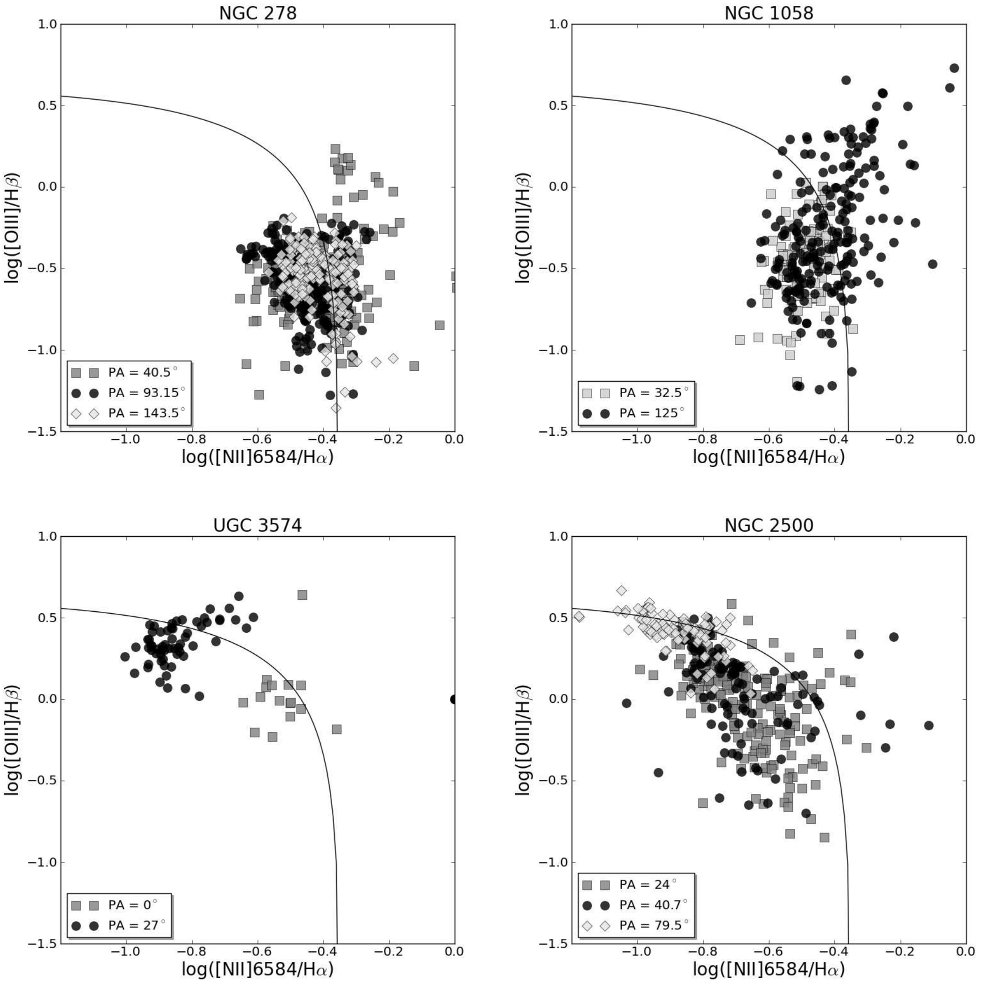

Fig. 3. Diagnostic Diagrams for the four galaxies of the sample, for the most commonly used [NII]/Hα vs. [OIII]/Hβ diagram (Veilleux & Osterbrock 1987). Photoionization appears to be the main ionizations mechanism, although there are some regions of low velocity shocks.

spiral density wave in a thick and magnetized gaseous disk, described by the Martos & Cox (1998) and Martos et al. (1999) galactic bore models.

Moreover other different patterns that can be found. There are Hα emission peaks clearly associated with a spiral arm, where the above pattern is not so clear. Besides, we also found important vertical displacements which are not related with high emission peaks. However we cannot discard these are not related with a spiral arm, since the leak or weakness in Hα emission do not determine the presence of a spiral arm. An outstanding example of this case is found in NGC 278, at PA = 143.5° - approximately the minor axis of the galaxy- see Fig. 2.

One possible interpretation for the approaching and receding peaks in ΔV_Z could be the deceleration and acceleration respectively of the rotational velocity. But in this case, where the slit position angles lies onto or close to the minor axis, the contribution of the rotational velocity is nearly negligible, and it is not able to explain the variations in the observed velocities, and therefore in V_Z. If V_Z were not considered, the observed velocity should be explained only by the rotational velocity. But a variation in the observed velocities $\Delta V_{obs} \sim 22$ kms^{-1}, between the galactocentric distances of 0.5 and 0.8 kpc , cannot be explained by the difference between the rotation velocities $\Delta V_{rot} \cos\theta \sin i \sim 0.13$ kms^{-1}(See Fig. 2). On the other hand, for a ΔV_{obs} of 22 kms^{-1}, due to its corresponding projection factor $\cos\theta \sin i \simeq -9E^{-3}$ (see Eq.[1]), it were required a ΔV_{rot} of the order of 2400 kms^{-1}, between distances of 300 pc. This same argument can be applied for the rest of galaxies.

To complete this kinematic analysis, Diagnostic Diagrams (DD) are included to determine the ionizing mechanisms in the observed features. Looking for shocks in all the zones where it is identified the pattern described by Martos & Cox (1998). The encounter of the gas with the density waves and on the assumption of hydraulic jumps, some traces of shocks should be found. It has been applied the well-known emission line ratios [NII]/Hα vs. [OIII]/Hβ (Baldwin, Philips & Terlevich 1981; Veilleux & Osterbrock 1987). The flux ratios are corrected from reddening before plotting the DD, applying the Balmer decrement and the Cardelli et al.(1989) extinction curve with $R_V = 3.1$.

Fig. 3 shows the DD for each galaxy. The different slit position angles for each galaxy are represented with different symbols and gray color scale, as it is indicated in the left-down panels. We do not observe clear traces of shocks in all the zones where it is identified the commented pattern above. In the case of NGC 278, traces of shocks appear only in the central zone, where it report the presence of a recent minor merger (Knapen et al. 2004). We can observed as photoionization, from high energetic photons, seems to be the main ionization mechanism. There is also a small portion of the gas that appears to be ionized by low-velocity shocks. In NGC 1058, for the slit with PA= 125°, this portion is more important. We also find and two differentiated behaviour in the DD. NGC 278 and NGC 1058 have most of their pixels, for the three slit positions, concentrated at the same location in the DD. Whereas for NGC 2500 and UGC 3574 each slit position occupies a different location in the DD, nearly covering the theoretical curve separating the different ionization mechanisms, as it were related with a metallicity gradient.

5. Summary

The existence of corrugations has been already reported, e.g. Alfaro et al. (2001), Matthews & Uson (2008). In this work not only the existence of radial and azimuthal corrugations are clearly observed, we report a first systematic study on the velocity corrugations in a sample of nearly face-on spiral galaxies. At this work we show a brief description of the morphologies or patterns found at these plots for each galaxy, which interpretation is still an open matter of discussion. We found different behaviors of the vertical velocity component respect to the Hα emission peaks, for our galaxy sample. In the Diagnostic Diagrams analysis, no clear traces of shocks are found. Photoionization is the main ionization mechanism in all these galaxies, and only a small portion of the gas appears to be ionized by low-velocity shocks. We also get a differentiation among the galaxies, NGC 278 and NGC 1058, by one hand, and NGC 2500 and UGC 3574, in the other, in their ionization behavior in the DD.

The origin of the corrugations is still matter of debate. Corrugations are closely link, as cause/effect, to the large scale star formation processes: density waves, tidal interactions, collisions of high velocity clouds with disk, or a galactic bore generated by the interaction of a spiral density wave with a thick gaseous disk, as modeled by Martos & Cox (1998), Martos et al. (1999), etc. Which mechanism is the origin of disk corrugations is still an open problem.

References

Alfaro, E. J., Cabrera-Cano, J., & Delgado, A. J. 1992, ApJ, 399, 576
Alfaro, E. J., & Efremov, Y. N. 1996, Revista Mexicana de Astronomia y Astrofisica Conference Series, 4, 1
Alfaro, E. J., et al., 2001, ApJ, 550, 253
Baldwin, J. A., Phillips, M. M., & Terlevich, R. 1981, PASP, 93, 5
Cardelli, J. A., Clayton, G. C., & Mathis, J. S. 1989, ApJ, 345, 245
Djorgovski, S., & Sosin, C. 1989, ApJL, 341, L13
de Vaucouleurs, G., & de Vaucouleurs, A. 1963, ApJ, 137, 363
Epinat, B., et al. 2008, MNRAS, 388, 500
Florido, E., et al., 2001, A&A, 378, 82
James, G., et al. 2004, A&A, 427, 825
Knapen, J. H., Whyte, L. F., de Blok, W. J. G., & van der Hulst, J. M. 2004, A&A, 423, 481
Lockman, F. J. 1977, BAAS, 9, 301
Malhotra, S., & Rhoads, J. E. 1995, The Formation of the Milky Way, 87
Martos, M. A., & Cox, D. P. 1998, ApJ, 509, 703
Martos, M., Allen, C., Franco, J., & Kurtz, S. 1999, ApJL, 526, L89
Matthews, L. D., & Uson, J. M. 2008, ApJ, 688, 237
Morton, D. C. 1965, ApJ, 141, 73
Moustakas, J., & Kennicutt, R. C., Jr. 2006, ApJS, 164, 81
Pişmiş, P. 1965, Boletin de los Observatorios Tonantzintla y Tacubaya, 4, 8
Quiroga, R. J. 1977, Ap&SS, 50, 281
Rhoads, J. E. 1995, Bulletin of the American Astronomical Society, 27, 1415
Spicker, J., & Feitzinger, J. V. 1986, A&A, 163, 43
Veilleux, S., & Osterbrock, D. E. 1987, ApJS, 63, 295